at -129.3 ppm, with two pairs of satellites corresponding to $^2J_{W-W}$ corner coupling is assigned to the W(6)-W(9) atoms. Because of its relative sharpness ($\Delta\nu_{1/2}$ = 20 Hz) and of its high frequency[13] the line at -100 ppm arises from the equivalent W(10)-W(11) atoms only edge coupled to vanadium. The two very broad low frequency resonances are from the W(1)-W(2) and W(7)-W(8) pairs, which are both corner-coupled with vanadium atoms. Precise assignment of these lines cannot be proposed on the basis of the present data.

Conclusion

This study establishes that the nature of the isomerization products of the γ(1,2)-$[SiV_2W_{10}O_{40}]^{6-}$ polyanion is strongly dependent on the experimental conditions, especially on the pH of the aqueous solution. Since the γ-isomer is stable in nonaqueous solution, the isomerization proceeds via hydrolitic cleavage of W-O or/and V-O bonds. In all cases, β-$[SiV_2W_{10}O_{40}]^{6-}$ isomers were obtained and appear then to be more resistant to hydrolysis, in basic as well as in acid solution, than the γ-structure, which is characterized by a bis(μ-oxo) bond between the vanadium atoms.

We are not able to derive precisely the mechanism of this hydrolytic reaction, but it appears to depend strongly on the nature, number, and protonation state of the oxo bridges between the metallic atoms concerned by the reaction. For example, a protonated form of the γ-complex is easily obtained in acid solution and evolves mainly to the β(3,12)-isomer. On the contrary, the unprotonated complex γ(1,2)-$[SiV_2W_{10}O_{40}]^{6-}$ appears to be stable (or very kinetically inert) in solution ($3 < pH < 5$). At higher pH, there are probably selective cleavages of V-O-V or/and V-O-W bonds, leading to unstable species that rearrange to give the more stable β-complexes.

Acknowledgment. We are grateful to a reviewer for suggesting the incorporation of Scheme I, which summarizes the interconversion processes.

Contribution from the Anorganisch-Chemisches Institut, Westfälische Wilhelms-Universität Münster, Wilhelm Klemm Strasse 8, D-4400 Münster, Federal Republic of Germany, Spectrochimie du Solide, Université Pierre et Marie Curie, 4 Place Jussieu, 75252 Paris Cedex 05, France, Systemes Energetiques et Transferts Thermiques, Université de Provence, Centre de Saint-Jerôme, Case 152, Avenue Escadrille Normandie-Niemen, 13397 Marseille Cedex 13, France, and Molten Salts Group, Chemistry Department A, Building 207, The Technical University of Denmark, DK-2800 Lyngby, Denmark

Crystallographic and ^{27}Al NMR Study on Premelting Phenomena in Crystals of Sodium Tetrachloroaluminate

Bernt Krebs,[†] Horst Greiwing,[†] Claus Brendel,[†] Francis Taulelle,[‡] Marcelle Gaune-Escard,[§] and Rolf W. Berg*[,∥]

Received May 14, 1990

The crystal structure of $NaAlCl_4$ was determined in the orthorhombic space group $P2_12_12_1$ (D_2^4, No. 19; Z = 4) at temperatures 138, 150, and 154 ± 0.2 °C, resulting in the lattice parameters a = 10.442 (4), 10.449 (3), 10.455 (2) Å, b = 9.973 (3), 9.993 (2), 10.002 (2) Å, and c = 6.202 (2), 6.206 (2), 6.204 (2) Å, respectively. Samples of the compound were investigated by differential scanning calorimetry. ^{27}Al NMR spectra were obtained on $NaAlCl_4$ and $LiAlCl_4$ solids as a function of temperature up to and above the melting points, at 157 and 146 °C, respectively. In accordance with the enhanced premelting heat contents, the observed phenomena indicate the existence of a specific dynamical behavior of the components in the two crystals, involving reorientational noncontinuous movements of the $AlCl_4^-$ ions and translational jumps of the alkali-metal cations.

Introduction

In a study[1] of the phase diagram of the NaCl-$AlCl_3$ system, the enthalpy of melting was determined cryoscopically to be about 15.5 kJ mol^{-1}. However, much higher values have been obtained calorimetrically: Rogers[2] found 19.4 ± 0.4 kJ mol^{-1}, and Denielou et al.[3] found 20.3 ± 0.5 kJ mol^{-1}. Also, in an impressive paper, Dewing[4] reported the enthalpy of liquid $NaAlCl_4$ versus temperature and obtained a ΔH_f value of 18.4 kJ mol^{-1}. These calorimetric values are so close that they are probably correct within ±2.0 kJ mol^{-1}. Due to the internal consistency, according to Dewing,[4] no serious error should exist in any of his final thermodynamic quantities (including ΔH_f).

The apparent disagreement between the values determined by cryoscopy and calorimetry has been considered[1] to be due to a possible structural change (premelting) in $NaAlCl_4$, around 140-150 °C. Upon heating (see Figure 1), the experimental enthalpy content of solid $NaAlCl_4$ follows a linear trend up to a temperature T_p of around 137 °C, from which temperature it starts to deviate positively. Apparently, the solid absorbs excessive heat of ΔH_p = ca. 4.5 kJ mol^{-1} until finally, at the melting point (T_f = ca. 156.7 °C), it absorbs the cryoscopically determined heat of ca. 15.5 kJ mol^{-1}.

Table I. Crystallographic Data for Sodium Aluminum Chloride

chem formula: $NaAlCl_4$
a = 10.442 (4), 10.449 (3), 10.455 (2) Å
b = 9.973 (3), 9.993 (2), 10.002 (2) Å
c = 6.202 (2), 6.206 (2), 6.204 (2) Å
$\alpha = \beta = \gamma$ = 90°
V = 645.9, 648.0, 648.8 Å^3
Z = 4
ρ_{calcd} = 1.972, 1.966, 1.963 g cm^{-3}
fw = 191.78
space group: $P2_12_12_1$ (D_2^4) (No. 19)
T = 138, 150, 154 °C
λ(Mo Kα) = 0.71069 Å
μ = 18.8 cm^{-1}
abs cor: none
$R(F_o)$ = 0.0350, 0.0442, 0.0476
$R_w(F_o^2)$ = 0.0342, 0.0425, 0.0403

To study this assumed premelting effect, we have now determined the structure of $NaAlCl_4$ single crystals by means of X-ray diffraction, just below the melting point. Previously, the structure has been solved at ambient temperatures[5-8] and at 125 °C.[9] Also,

[†] Westfälische Wilhelms-Universität Münster.
[‡] Université Pierre et Marie Curie.
[§] Université de Provence.
[∥] The Technical University of Denmark.

(1) Berg, R. W.; Hjuler, H. A.; Bjerrum, N. J. *Inorg. Chem.* **1984**, *23*, 557.
(2) Rogers, L. J. *J. Chem. Thermodyn.* **1980**, *12*, 51.
(3) Denielou, L.; Petitet, J.-P.; Tequi, C. *J. Chem. Eng. Data* **1982**, *27*, 129.
(4) Dewing, E. W. *Metall. Trans. B* **1981**, *12B*, 705.
(5) Baenziger, N. C. *Acta Crystallogr.* **1951**, *4*, 216.
(6) Scheinert, W.; Weiss, A. *Z. Naturforsch., A* **1976**, *31A*, 1354.

0020-1669/91/1330-0981$02.50/0

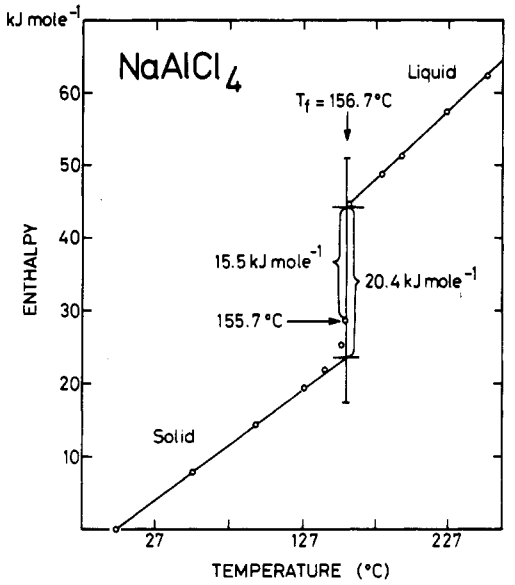

Figure 1. Enthalpy of $NaAlCl_4$ as a function of temperature ($H_{273\,K}$ = 0). The experimental points are due to Denielou et al.[3] Note the H value on the solid curve only 1 °C below the melting point at 156.7 °C.

we have studied the ^{27}Al NMR response of $NaAlCl_4$ and $LiAlCl_4$ versus temperature across the melting range.

Experimental Section

Preparation of Samples. Drybox and vacuum-line techniques were employed, due to the sensitivity of the compounds to water. $LiAlCl_4$ and $NaAlCl_4$ of highest attainable purities[1] were used, prepared from equimolar amounts of $AlCl_3$ (Fluka, puriss, sublimed and distilled twice[1]) and pure LiCl or NaCl. These chemicals were fused together in an ampule, followed by recrystallization, decantation, and zone-refining. Only colorless clear crystals were used, sealed into X-ray, NMR, or calorimetric sampling tubes or put into closed aluminum DSC crucibles.

The structural results (Table I) were obtained with a four-circle Syntex $P2_1$ diffractometer using graphite-monochromated Mo Kα radiation and operating in the θ–2θ scanning mode ($4° < 2\theta <$ ca. 60°) at intensity-dependent rates of 5–30° min^{-1}. Three different single crystals of sizes 300 × 300 × 50, 150 × 200 × 70, and 200 × 300 × 50 μm, respectively, were used at three different temperatures 138, 150, and 154 °C. The temperatures (±0.2 °C) were obtained by a stream of warm air, from an ENRAF-NONIUS FR559 heating device that has been modified to increase temperature stability and reproducibility. A total of 844, 1120, and 1123 reflections were collected. The cell constants at each temperature were refined from 15 high-order reflections by least-squares methods. No correction for absorption was done. The structure refinement was started from the already known structure at 125 °C in space group $P2_12_12_1$[9] by using 709, 837, and 685 reflections having $I > 1.96\sigma(I)$, respectively. The refinement method involved anisotropic full-matrix least-squares minimization using the Syntex EXTL and the SHELXTL computer programs.[10] Atomic scattering factors were taken from ref 11. Observed and calculated structure factors are given in supplementary material Tables SI–SIII.

Thermal Experiments. The thermal behavior of $NaAlCl_4$ was studied by using two techniques, differential scanning calorimetry and differential enthalpic analysis.

A differential scanning calorimeter (Perkin-Elmer DSC 4) employed aluminum closed crucibles and samples with a small mass (a few milligrams). Heatings and coolings were done at relatively fast rates, between 10 and 30 °C min^{-1}.

Differential enthalpic analysis experiments were conducted in a Calvet type calorimeter. The samples (several grams) were loaded in sealed quartz ampules. Heating/cooling rates were moderately low (10 °C h^{-1}). This technique, already used to investigate compounds undergoing several phase transitions, is very sensitive and makes it possible to separate thermal effects due to transitions occurring at very close temperatures.[12-16] Calibration was done with indium.

High-Resolution NMR Measurements were carried out on a multinuclear Bruker CXP-300 spectrometer, operating at 7.05 T with the Fourier transform technique and the ^{27}Al resonance frequency of 78.2 MHz. NMR spectra were recorded at different temperatures. Below 100 °C an aqueous solution, 1.0 M in $Al(NO_3)_3$ and 1.0 M in HNO_3, was used as the external reference for the chemical shifts (taken as positive for signals on the low-field side). The variation of the chemical shift of the reference with temperature was negligible, and this was also assumed to be the case for measurements above 100 °C. Other experimental details are given in ref 17.

Table II. $NaAlCl_4$: Positional Parameters of the Atoms and U_{eq} Values in $Å^2$ with Estimated Standard Deviations[a]

atom	temp, °C	x/a	y/b	z/c	U_{eq}
Na	20*	0.1252 (2)	0.2132 (2)	0.6889 (4)	0.068 (1)
	80*	0.1256 (2)	0.2143 (2)	0.6885 (4)	0.091 (1)
	120*	0.1258 (3)	0.2150 (3)	0.6889 (6)	0.105 (1)
	138	0.1258 (4)	0.2146 (2)	0.6889 (6)	0.115 (2)
	150	0.1256 (5)	0.2154 (4)	0.6884 (7)	0.121 (2)
	157	0.1262 (4)	0.2153 (4)	0.6888 (6)	0.121 (1)
Al	20*	0.0378 (1)	0.4858 (2)	0.2069 (2)	0.030 (1)
	80*	0.0377 (1)	0.4857 (1)	0.2050 (2)	0.039 (1)
	120*	0.0377 (1)	0.4859 (1)	0.2032 (2)	0.045 (1)
	138	0.0377 (1)	0.4859 (1)	0.2032 (3)	0.047 (1)
	150	0.0376 (2)	0.4860 (2)	0.2027 (3)	0.048 (1)
	157	0.0377 (2)	0.4860 (2)	0.2025 (3)	0.050 (1)
Cl(1)	20*	0.0322 (1)	0.4913 (1)	0.5524 (2)	0.042 (1)
	80*	0.0318 (1)	0.4913 (1)	0.5491 (2)	0.055 (1)
	120*	0.0313 (1)	0.4913 (1)	0.5465 (2)	0.063 (1)
	138	0.0314 (2)	0.4912 (2)	0.5457 (2)	0.066 (1)
	150	0.0310 (2)	0.4914 (2)	0.5453 (3)	0.069 (1)
	157	0.0311 (2)	0.4916 (2)	0.5446 (3)	0.071 (1)
Cl(2)	20*	0.1481 (1)	0.3145 (1)	0.1092 (2)	0.043 (1)
	80*	0.1475 (1)	0.3156 (1)	0.1081 (2)	0.056 (1)
	120*	0.1469 (1)	0.3165 (1)	0.1072 (2)	0.065 (1)
	138	0.1468 (2)	0.3167 (2)	0.1066 (3)	0.068 (1)
	150	0.1469 (2)	0.3167 (2)	0.1067 (4)	0.071 (1)
	157	0.1466 (2)	0.3171 (2)	0.1061 (3)	0.072 (1)
Cl(3)	20*	0.3465 (1)	0.0226 (1)	0.9253 (2)	0.042 (1)
	80*	0.3479 (1)	0.0227 (1)	0.9273 (2)	0.056 (1)
	120*	0.3489 (1)	0.0222 (1)	0.9288 (2)	0.065 (1)
	138	0.3492 (2)	0.0226 (2)	0.9291 (3)	0.067 (1)
	150	0.3494 (2)	0.0219 (2)	0.9298 (3)	0.070 (1)
	157	0.3495 (2)	0.0223 (2)	0.9296 (3)	0.072 (1)
Cl(4)	20*	0.3774 (1)	0.3353 (1)	0.5735 (2)	0.041 (1)
	80*	0.3777 (1)	0.3360 (1)	0.5726 (2)	0.055 (1)
	120*	0.3778 (1)	0.3363 (1)	0.5725 (2)	0.063 (1)
	138	0.3777 (2)	0.3367 (2)	0.5724 (3)	0.067 (1)
	150	0.3776 (2)	0.3367 (2)	0.5721 (4)	0.070 (1)
	157	0.3773 (2)	0.3370 (2)	0.5722 (3)	0.071 (1)

[a] U_{eq} is defined as one-third of the trace of the orthongalized U_{ij} tensor. Data given by Perenthaler et al.[9] are indicated by asterisks.

Results and Discussion

Structural Results. Crystal data and other details are given in Table I. The final X-ray data are of highest possible precision, attainable with the existing experimental setup, with which we cannot get closer to the melting point (X-ray diffraction studies on $LiAlCl_4$ and $NaAlCl_4$ melts are available[18,19]). The obtained

(7) Wallart, F.; Lorriaux-Rubbens, A.; Mairesse, G.; Barbier, P.; Wignacourt, J. P. *J. Raman Spectrosc.* **1980**, *9*, 55.
(8) Mairesse, G.; Barbier, P.; Wignacourt, J. P. *Acta Crystallogr., Sect. B* **1979**, *B35*, 1573.
(9) Perenthaler, E.; Schulz, H.; Rabenau, A. *Z. Anorg. Allg. Chem.* **1982**, *491*, 259.
(10) Sheldrick, G. M. EXTL program package. Syntex Co., Cupertino, CA. SHELXTL program. University of Göttingen, 1981.
(11) *International Tables for X-Ray Crystallography*; Kynoch Press: Birmingham, England, 1974; Vol. IV, p 99.
(12) Fouque, Y.; Gaune-Escard, M.; Szczepaniak, W.; Bogacz, A. *J. Chim. Phys.* **1978**, *75*, 360.
(13) Bogacz, A.; Wisniowski, M.; Fouque, Y.; Bros, J.-P.; Gaune-Escard, M. *J. Cal. Anal. Therm.* **1983**, *XIV*, 339.
(14) Bogacz, A.; Szczepaniak, W.; Bros, J.-P.; Fouque, Y.; Gaune-Escard, M. *J. Chem. Soc., Faraday Trans. 1* **1984**, *80*, 2935.
(15) Fouque, Y.; Bros, J.-P.; Gaune-Escard, M.; Wisniowski, M.; Bogacz, A. *Ber. Bunsen-Ges. Phys. Chem.* **1985**, *89*, 777.
(16) Bros, J.-P.; Gaune-Escard, M.; Szczepaniak, W.; Bogacz, A.; Hewat, A. W. *Acta Crystallogr., Sect. B* **1987**, *43B*, 113.
(17) Taullele, F.; Popov, A. I. *J. Solution Chem.* **1986**, *15*, 463.
(18) Takahashi, S.; Maruoka, K.; Koura, N.; Ohno, H. *J. Chem. Phys.* **1986**, *84*, 408.

Table III. Interatomic Distances (Å) for $NaAlCl_4$ at 0, 80, 120, 138, 150, and 154 °C with Estimated Standard Deviations[a]

	temp, °C						
	20[b]	80[b]	120[b]	138	150	154	154
Al–Cl(1)[a]	2.132 (3)	2.129 (3)	2.129 (3)	2.127 (2)	2.128 (2)	2.125 (2)	[2.140][c]
Al–Cl(2)	2.127 (2)	2.124 (2)	2.120 (2)	2.127 (3)	2.125 (3)	2.122 (3)	[2.137]
Al–Cl(3A)	2.136 (2)	2.135 (2)	2.130 (2)	2.136 (2)	2.133 (3)	2.133 (2)	[2.150]
Al–Cl(4B)	2.138 (2)	2.140 (2)	2.137 (2)	2.140 (3)	2.141 (3)	2.139 (3)	[2.153]
Na–Cl(1)	3.031 (3)	3.043 (3)	3.054 (4)	3.067 (4)	3.062 (5)	3.069 (4)	
Na–Cl(3)	3.299 (3)	3.336 (3)	3.360 (4)	3.369 (4)	3.384 (5)	3.379 (4)	
Na–Cl(4)	2.995 (3)	2.971 (3)	2.977 (4)	2.990 (5)	2.987 (5)	2.982 (4)	
Na–Cl(1A)	3.161 (3)	3.195 (3)	3.214 (4)	3.224 (4)	3.228 (5)	3.234 (4)	
Na–Cl(2A)	2.788 (4)	2.792 (4)	2.791 (4)	2.794 (4)	2.795 (5)	2.792 (4)	
Na–Cl(3B)	2.857 (3)	2.868 (3)	2.873 (4)	2.878 (4)	2.875 (5)	2.879 (4)	
Na–Cl(4A)	3.063 (3)	3.072 (4)	3.093 (4)	3.101 (5)	3.099 (5)	3.108 (4)	

[a] The atoms Cl(1A), Cl(2A), Cl(3A), and Cl(4A) as well as Cl(3B) and Cl(4B) are symmetrically equivalent with the atoms Cl(1)–Cl(4) in Table II. The corresponding symmetry operations of the $P2_12_12_1$ space group are as follows: (A) $0.5 + x, 0.5 - y, -z$; (B) $0.5 - x, -y, 0.5 + z$. [b] Data by Perenthaler et al.[9] [c] Values obtained from the librational analysis are given inside brackets.

Table IV. $NaAlCl_4$: Bond Angles (deg) in $AlCl_4^-$ Tetrahedra with Estimated Standard Errors[a]

	temp, °C		
	138	150	154
Cl(1)–Al–Cl(2)	108.5 (1)	108.5 (1)	108.6 (1)
Cl(1)–Al–Cl(3A)	110.9 (1)	110.9 (1)	110.8 (1)
Cl(1)–Al–Cl(4B)	111.8 (1)	111.7 (1)	111.7 (1)
Cl(2)–Al–Cl(3A)	110.7 (1)	111.0 (1)	110.8 (1)
Cl(2)–Al–C(4B)	109.3 (1)	109.3 (1)	109.2 (1)
Cl(3A)–Al–Cl(4B)	105.6 (1)	105.4 (1)	105.7 (1)

[a] The angles given by Perenthaler et al.[9] for their results at 20 and 120 °C are in accordance with our values within the specified error limits.

positional and isotropic structural parameters are given as a function of temperature in Table II, including results previously published (marked with asterisks).[9] Anisotropic temperature factors U_{ij} and the anisotropic temperature factor expression are given in supplementary material Table SIV.

The conventionally refined occupational factor for sodium was 0.97 (1), determined by using atomic scattering factors, but it can be brought to ca. 1.00 (1) by use of ionic scattering factors for Na^+ and different ionic models between $Al^+(Cl^{1/2-})_4$ and $Al^{2+}(Cl^{3/4-})_4$ for chloroaluminate. There is no significant influence of the assumed charge distribution in the anion on this value of 1.00 for Na^+. The data in Tables II–IV and supplementary material Tables SIV–SV refer to the model $Na^+Al^+(Cl^{1/2-})_4$. Hence, the underoccupation for sodium, discussed by Perenthaler et al.,[9] probably is an artifact due to use of scattering factors for neutral atoms in a partly ionic, partly molecular crystal. Analysis of the final high-resolution electron density difference maps did not give any hints of residual unaccounted charges.

The large isotropic temperature factors, also for sodium, are smoothly linear continuations of the values obtained at much lower temperatures; see Figure 2a. Similar plots were obtained for the vibrational amplitudes for sodium (principal axes of the thermal vibrational ellipsoids); see Figure 2b.

The obtained atomic distances were corrected for errors due to rigid-body librations by the method of Schomaker and Trueblood.[20] In this way, the Al–Cl distances increased from within 2.122 (3) and 2.139 (3) Å to within 2.137 (3) and 2.153 (3) Å, i.e. by ca. 0.015 (3) Å. All obtained interatomic distances and angles are given in Tables III and IV, respectively, as a function of temperature (the Al–Cl distances obtained by the librational analysis at 154 °C are given inside brackets). The **L** and **T** tensors from the librational analysis are given in supplementary material Table SV.

Description and Discussion of the Structure. The $NaAlCl_4$ salt crystallizes as plates or prisms in a deformed baryte type structure[5,8,9,21] and is known to have a structure very similar to that of $NaFeCl_4$,[22] with which it forms solid solutions.[23] The space group is $P2_12_12_1$ with four formula units in the orthorhombic cell. All atoms are on general positions. The structure consists of isolated slightly distorted tetrahedral $AlCl_4^-$ anions, which are separated by Na^+ cations, as shown in Figure 3. Each tetrahedron has an orientation such that one face is approximately parallel

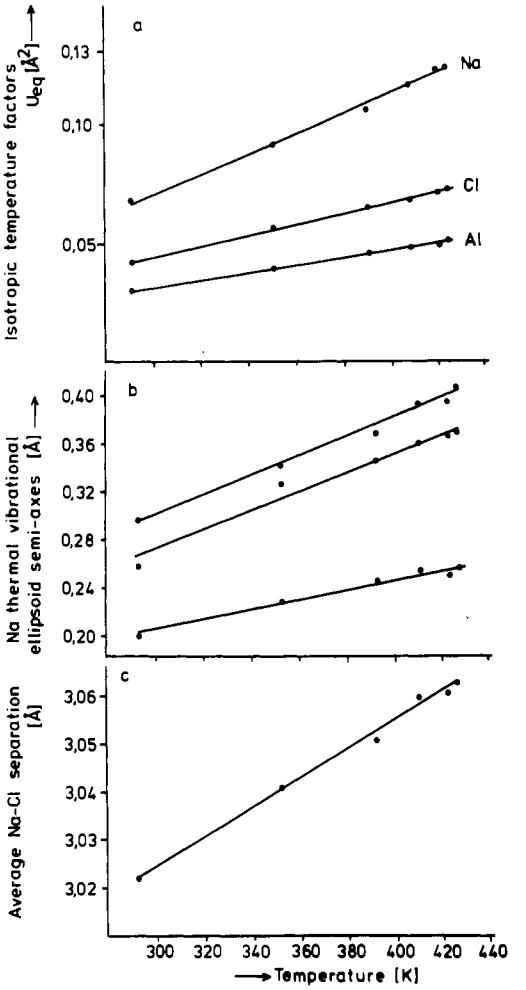

Figure 2. Temperature dependence of (a) isotropic temperature factors (U_{eq}), (b) semiaxes of thermal ellipsoids for Na^+, and (c) average Na–Cl separations. All curves show smoothly linear trends. For Cl, average U_{eq} values of the four individual temperature factors are given.

(19) Takahashi, S.; Muneta, T.; Koura, N.; Ohno, H. *J. Chem. Soc., Faraday Trans. 2* **1985**, *81*, 319 and 1107.
(20) Schomaker, V.; Trueblood, K. N. *Acta Crystallogr., Sect. B* **1968**, *24B*, 63.
(21) Mayer, G.; Schwan, E. *Z. Naturforsch., B* **1980**, *35B*, 117.
(22) Richards, R.; Gregory, N. W. *J. Phys. Chem.* **1965**, *69*, 239.
(23) Spiesser, M.; Palvadeau, P.; Guillot, C.; Cerisier, J. *Solid State Ionics* **1983**, *9*, *10*, 103.

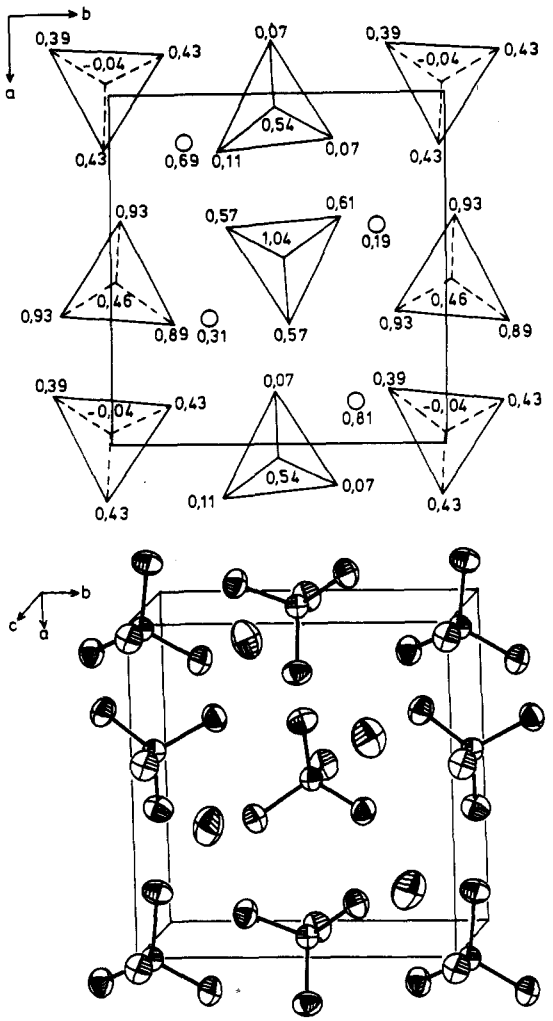

Figure 3. Unit cell of $NaAlCl_4$: (a, top) Projection of atoms along *c* with fractional *z* coordinates given; (b, bottom) unit cell with all atoms given as ellipsoids of 50% probability of containment.

to the (001) plane and the opposing Cl atom is pointing alternatingly in the positive and the negative direction of the *c* axis. Alternatively, the structure can be described as a close-packed Cl network with some voids filled with Al and Na.

The conventionally refined distances between Al and Cl in the $AlCl_4^-$ tetrahedron are within 2.122 and 2.139 Å at 154 °C. Similar ranges are found at other temperatures and are quite normal; e.g., ca. 2.13 and 2.14 Å were found for $KAlCl_4$[24] and SCl_3AlCl_4,[25,26] respectively. In $NaAlCl_4$, the bond angles between Al and Cl deviate up to ±3.8° from the ideal tetrahedral angle, the deformation not being affected very much by change in temperature. This deformation is smaller than for $KAlCl_4$ (which is up to ca. 7.7°[24]) and larger than for SCl_3AlCl_4 (up to ca. ±2°[25,26]).

As is to be expected when close to the melting temperature, the atoms perform large, though not unusually large, thermal movements. The temperature factors obtained during the refinements (supplementary material Table SIV) and the thermal ellipsoids (Figure 2) clearly indicate, however, that at first sight neither the translational movement of Na^+ nor the librational motions of the $AlCl_4^-$ tetrahedra are excessive. The tetrahedra are far from being in a state of free rotational motion. By the plotting of temperature factors versus temperature (see Figure 2), linear dependencies are obtained for the Al, Cl, and Na atoms, and the slope is clearly larger for Na.

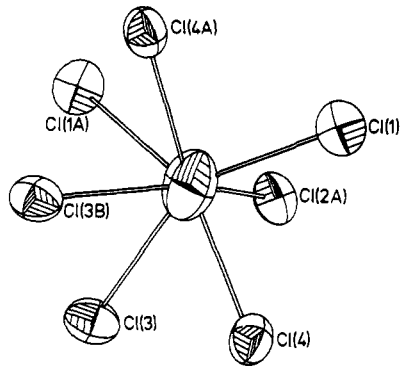

Figure 4. Coordination geometry around sodium in the $NaAlCl_4$ structure. Ellipsoids show 50% probability of containment.

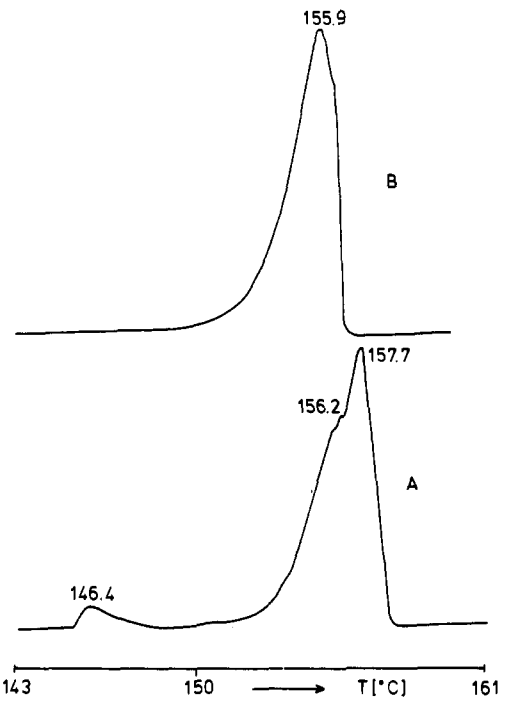

Figure 5. Thermograms obtained by differential scanning calorimetry (endothermic signals upward): (A) Curve obtained during first heating of the sample; (B) curve obtained after melting and solidification.

A comparison of the structures at six different temperatures shows that the positional parameters of the individual atoms constitute a small continuous translation of the tetrahedron as a whole (see *z* coordinate of aluminum). The increase in Na–Cl separation with temperature, already reported by Perenthaler et al.,[9] is continued at the temperatures investigated here, although there is no significant increase anymore between 138 and 154 °C (Figure 2c).

The surroundings of Na^+ are characterized by an irregular, 7-fold coordination of chloride (see Figure 4). The Na–Cl distances vary from 2.79 to 3.38 Å (Table III). The irregular coordination of the cations has also been observed in higher alkali-metal tetrachloroaluminates (see discussion by Mairesse et al.[8]).

It must be added that high-temperature Weissenberg diagrams[27] have shown neither indication of a phase transition in $NaAlCl_4$ nor anomalous diffuse scattering effects in the temperature range from 140 °C up to its melting point (photographs taken in steps of 1 ± 0.1 °C).

Thermal Experiments. At the fusion temperatures, all thermoanalytic (DSC and calorimetric) experiments have shown strongly endothermic features that were markedly unsymmetric because of the premelting dynamical processes in the structure.

(24) Mairesse, G.; Barbier, P.; Wignacourt, J. P. *Acta Crystallogr., Sect. B* **1978**, *34B*, 1328.
(25) Krebs, B.; Hein, M.; Janssen, H. Unpublished data.
(26) Trojanow, S. I.; Kolditz, L.; Radde, A. *Z. Chem.* **1983**, *23*, 136.
(27) Hoffmann, W. personal communication.

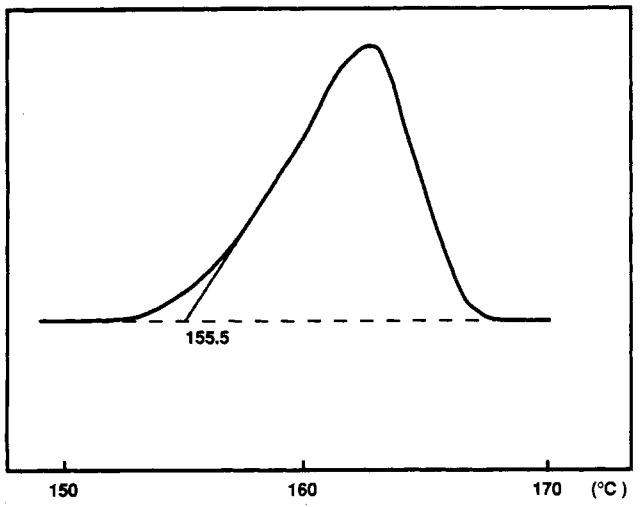

Figure 6. Differential enthalpic analysis thermogram obtained on heating of $NaAlCl_4$ (sample mass 3.370 g; heating rate 10 °C h^{-1}, endothermic signal upward).

Table V. Calorimetric Results (Average of First and Second Runs) for Fusion and Solidification

sample no.	wt, g	T_f, °C	T_s, °C	ΔH_f, kJ mol^{-1}	ΔH_s, kJ mol^{-1}
1	3.1980	156	*a*	21.01	*a*
2	3.3697	155	157–149	20.93	20.60
3	3.6189	152.5	*a*	20.97[b]	*a*
4[c]	3.6277	147 ± 1	148–152	21.56 ± 0.2	21.07

[a] No reliable value due to supercooling. [b] Small endothermic feature before melting the first time. [c] Probably not entirely pure sample.

In the initial (DSC) experiments in aluminum crucibles, a very small endothermic effect of <100 J/mol was observed at 146 °C during heating, prior to the *first* melting process, starting at 152.9 and ending at 157.7 °C (see Figure 5, curve A). The 146 °C peak was reproducible, but it appeared only during the first heating; it was gone when the same sample (after cooling) was heated a second time to obtain remelting (between 151.5 and 156.5 °C; see Figure 5, curve B). The peaks were also asymmetric in a manner that varied.

The calorimetric experiments were repeated in closed quartz ampules (Calvet calorimeter). A summary of the results is given in Table V, and a thermogram is shown in Figure 6. A small endothermic feature was detected on one sample at 152 °C, during the first run (not the one shown in Figure 6). This did not happen during the next run with the same sample or with the other samples (all three samples were run two times).

The fact that the effect was not seen in all cases may be interpreted to mean that it was caused by marginally different degrees of order, relaxing irreversibly, in the bulk or at the surface of the primary crystals, which have been produced under different (slower) crystallization conditions. A trivial effect of chemical impurities causing the presence of the endothermic peak is not likely, since it is in accord with the enthalpic and cryoscopic data.

NMR Spectra of Aluminum-27. General Theory. The excitation of a quadrupolar nucleus like ^{27}Al (nuclear spin I of $^5/_2$) is quite different in the liquid and solid state and differs from a usual NMR experiment. It is therefore necessary to consider the excitation function and its consequences on the quantitative analysis of the NMR signal, as explained in detail in ref 28 and references therein.

The transverse nuclear magnetization M_{xy} is the physical observable of the NMR experiment. It depends on the ratio ν_q/ν_1 and the duration t_{pulse} of the radio frequency pulse applied to the spin system, where ν_q and ν_1 are the quadrupolar and applied radio frequencies. Also, $\nu_q = (3/2I(2I-1))(e^2qQ/h)$, where h and e^2qQ/h are Planck's constant and the quadrupole coupling constant, respectively.

Two extreme cases may be observed: If ν_q/ν_1 is very small compared to 1 and if it is far greater than 1. In both cases, the response is approximately linear for small pulse durations. When maximum intensity is normalized to 1, the linear slope is 1 when ν_q/ν_1 is small compared to 1. A linear slope of $3(I + {}^1/_2)/4I(I + 1) = {}^9/_{35}$ for $I = {}^5/_2$ is obtained for the case where ν_q/ν_1 is greater than 1.

As a consequence, if the compound undergoes a solid- to liquid-phase transition in such a way that the local motion around the aluminum atoms is affected, then the average value of the quadrupolar interaction is modified. Therefore, at fusion the magnetization response will jump from one linear regime to another. However, even without fusion, if some averaging occurs e.g. due to rotational motion, here of $AlCl_4^-$, then the quadrupolar interaction may be reduced and some changes observed in the linear slope of the response. At a phase transition a change in the dielectric properties occurs, and additional effects may appear close to it. The dielectric properties of the sample may thus vary drastically, precisely when the passage of the phase transition takes place.[28] In such a case, the response of the system is affected by these variations, such that if the pulse duration is kept constant, the tip angle α of the magnetization is modified. So, quantification of the magnetization during the phase transition is precluded. However, before and after the phase transition, quantification of the magnetization can indeed be done by the Curie law. The latter states that the maximum magnetization observable $M_{ns}(\max)$ in the case of extreme narrowing, i.e. for the liquid state, can be expressed as

$$M_{ns}(\max) = N(\tau h)^2 I(I+1)H_0/3kT \qquad (1)$$

Here the symbols: ns, N, τ, I, H_0, k, and T stand respectively for nonselective, number of spins, correlation time, atomic spin quantum number, magnetic field applied to the system, Boltzmann's constant, and the absolute temperature. For a small tip angle, $\alpha = 2\pi\nu_1 t_{pulse}$, the expression becomes

$$M_s = M_{ns}(\max)\sin\alpha \qquad (2)$$

where s stands for selective. In the solid-state case, only a fraction of the total magnetization is observed according to Schmidt[29] (eq 3). In both cases, during an increase in temperature, the evolution

$$M_{obs} = \left(\frac{3(I+{}^1/_2)}{4I(I+1)}\right) M_{ns}(\max)\sin\alpha \qquad (3)$$

in magnetization obeys a relation in $1/T$. The multiplication factor of the $1/T$ function is not the same before and after the fusion.

^{27}Al NMR Spectral Results. NMR spectra of ^{27}Al have been obtained previously on various $AlCl_3$–MCl melts, e.g. with M = Li, Na, and K, as discussed in ref 17. For melts of 50 mol % of $AlCl_3$, a single narrow resonance line was observed at +103 ppm relative to the aluminum reference.[17] Also for $AlCl_4^-$ salts dissolved in $POCl_3$, ^{27}Al NMR spectra show a signal near 103 ppm.[30]

Our ^{27}Al results comprise the solid as well as the liquid phase for $NaAlCl_4$ and $LiAlCl_4$. The ^7Li and ^{23}Na spin–lattice relaxation times of the liquid phases have already been obtained.[31] Our data are plotted as a function of the temperature in Figures 7 and 8, respectively. As expected, a single broad line due to $AlCl_4^-$ is seen for the solid state and a narrow line for the liquid one, situated at ca. 103 ppm, in perfect agreement with previous results.[17]

The integral of a spectrum gives the nuclear magnetization at the appropriate temperature. The values calculated from the

(28) Taullele, F. NMR of Quadrupolar Nuclei in the Solid State. In *A Methodological Approach to Multi-nuclear Magnetic Resonance in Liquids and Solids: Chemical Applications*; NATO-ASI Summer School, Aug 1988, Maratea, Italy.

(29) Schmidt, V. H. *Proc. Ampere Int. Summer Sch.* **1971**, *2*, 75. Partly reproduced in: *Experimental Pulse NMR*; Fukushima and Roeder, Eds.; Addison-Wesley Publ. Co.: Reading, MA, 1981.

(30) Birkeneder, F.; Berg, R. W.; Hjuler, H. A.; Bjerrum, N. J. *Z. Anorg. Allg. Chem.* **1989**, *573*, 170.

(31) Matsumoto, T.; Ichikawa, K. *Nippon Kagaku Kaishi* **1982**, 1100; *Chem. Abstr.* **1982**, *97*, 65288x.

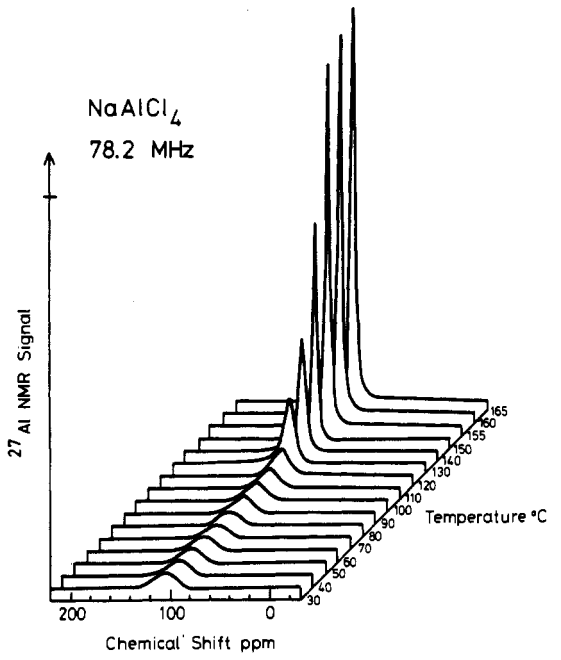

Figure 7. High-resolution ^{27}Al NMR spectra of $NaAlCl_4$ at various temperatures.

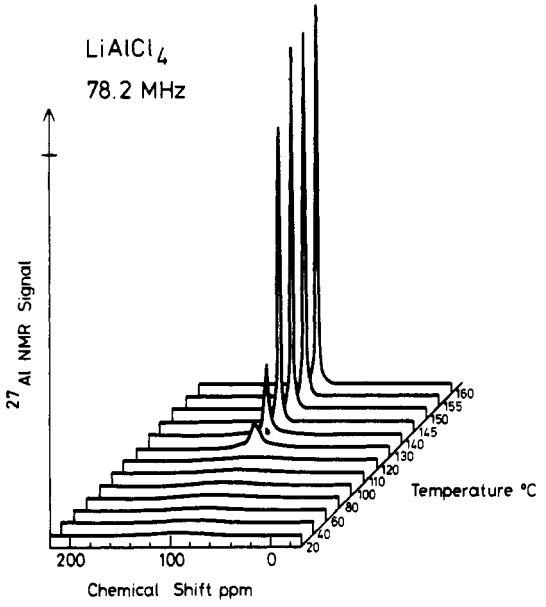

Figure 8. High-resolution ^{27}Al NMR spectra of $LiAlCl_4$ at various temperatures.

spectra have been plotted versus temperature in Figures 9 and 10, respectively. For $NaAlCl_4$ a Curie law is obtained from ambient temperature up to ca. 80 °C. Then the magnetization starts to increase and reaches $^{35}/_{9}$ of the selective irradiation obtained for the solid. Averaging of the quadrupolar interaction is completed at ca. 150 °C, before fusion. Then, during the fusion process the dielectric properties of the sample varies, changing the tuning of the resonator and giving some increase in the magnetization (the probe head goes from slightly detuned on the solid to tuned on the liquid). Then the Curie law is found again.

For $LiAlCl_4$ a behavior with two regions is found below ca. 110 °C. Below ca. 40 °C a Curie law is observed with the same slope as for $NaAlCl_4$. Between 40 and 80 °C we see a transition to a new line ranging from above ca. 80 °C and up to ca. 110 °C (i.e. here the same behavior as that for $NaAlCl_4$ is followed, except that the magnetization has been shifted by a fixed amount). From then on, a strong increase starts, though the quadrupolar interaction is not completely averaged out. Actually, at 140 °C the magnetization does not reach the expected value for a completely

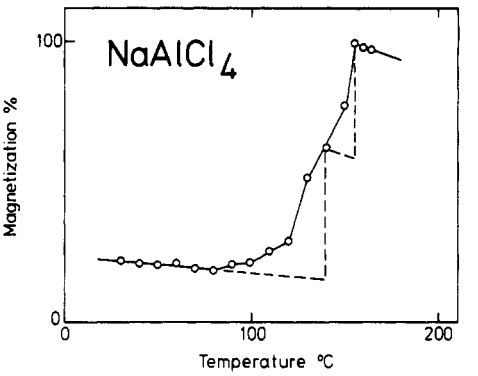

Figure 9. Plot of nuclear magnetization (area of the ^{27}Al NMR resonance) of $NaAlCl_4$ versus temperature.

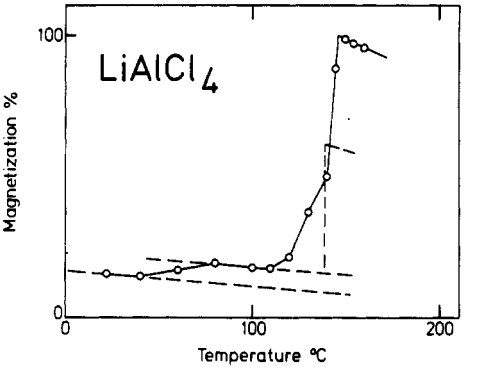

Figure 10. Plot of nuclear magnetization (area of the ^{27}Al NMR resonance) of $LiAlCl_4$ versus temperature.

averaged process. At fusion, a sharp increase occurs, under much the same conditions as those for $NaAlCl_4$.

The involved quadrupolar interaction acts around the aluminum nucleus. Averaging of this interaction means faster motion of the electronic field gradient at the aluminum nucleus. Such a motion is produced directly by the motion of the $AlCl_4^-$ tetrahedron as a whole. Therefore, the results for $NaAlCl_4$ could be described by a normal increase of vibrational and rotational modes of $AlCl_4^-$ up to ca. 80 °C and then followed by large-amplitude hindered rotation and finally initiation of rotation in the range from ca. 80 to 150 °C. At this temperature the magnetization reaches the theoretical value for a selective to nonselective excitation.

The situation in $LiAlCl_4$ may likewise be described as, first, a change in motion of lithium starting by ca. 40 °C and finishing at ca. 80 °C. Between ca. 80 and ca. 110 °C, $LiAlCl_4$ behaves like $NaAlCl_4$ does between room temperature and ca. 80 °C. Then, large-amplitude rotation of $AlCl_4^-$ begins. Fusion occurs before rotation of $AlCl_4^-$ starts, as indicated by the incomplete averaging of the quadrupolar interaction at the fusion point. As the liquid dielectric properties of $NaAlCl_4$ and $LiAlCl_4$ are about the same, the magnetization variation due to dielectric change leads to the same total magnetization at fusion.

The behavior between ca. 20 and ca. 40 °C indicates a lower symmetry of $AlCl_4^-$ in $LiAlCl_4$ than for $NaAlCl_4$ (see discussion in ref 8). The quadrupolar interaction is larger, and the NMR response lower. Then, between ca. 40 and 80 °C some motion starts leading to the same behavior for $AlCl_4^-$ in Li as in Na compounds. The rotation of $AlCl_4^-$ in the Li compound starts at higher temperatures than the corresponding phenomenon for the Na compound. This confirms a stronger interaction between $AlCl_4^-$ and the cation in the lithium case, as also observed previously.[32]

General Discussion

The results of the X-ray structure refinements indicate normal librational behavior of rather stationary $AlCl_4^-$ ions and no sig-

(32) Taulelle, F.; Popov, A. I. *Polyhedron* **1983**, *2*, 889.

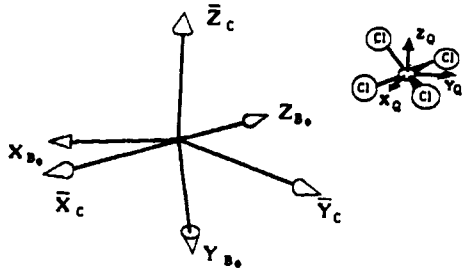

Figure 11. Representation of the three different axis systems necessary to describe an $AlCl_4^-$ ion during diffraction and magnetic resonance.

nificant excessive isotropic or anisotropic translational movements of the $AlCl_4^-$ or Na^+ species. A heating of the samples to above 146 °C does not produce any visible effect in the diffraction pattern (single crystal and powder). On the other hand, DSC curves have shown a weak endothermic peak at ca. 146 °C when the samples were heated to melt the first time, and the high-temperature ^{27}Al NMR spectra are explainable in terms of rotating $AlCl_4^-$ ions.

Furthermore, solid-state conductivity measurements and other kinds of evidence have shown a lot of motion for Na^+ and Li^+ in $NaAlCl_4$ and $LiAlCl_4$, respectively.[23,33-35] Also, ^7Li NMR spectra for solid $LiAlCl_4$ versus temperature have shown a dramatic line-width narrowing above about 100 °C, indicating that lithium is in a "liquidlike state" above about 100 °C.[23]

The contradiction between the X-ray diffraction method, which assumes the structure as stationary, and the NMR method, which senses the motion, is only apparent: Consider the microstructure of the $NaAlCl_4$ crystal. The description of an $AlCl_4^-$ ion requires three different axis systems from an X-ray diffraction point of view and from an NMR point of view (see Figure 11). The subscripts indicate whether it is a crystallographic axis system (C), an NMR laboratory frame axis system (B_0), or the quadrupolar principal axis system (Q).

The averaging process taking place in an NMR experiment implies a motion of Q relative to B_0. If this is so, one should observe an increase in the size of the positional ellipsoids measured by X-ray diffraction. We know that Li^+ and Na^+ can jump, since the compounds are highly ionic conducting solids.[23,33-35] The mean position seen by X-ray diffraction is actually the statistical average of different positions. We do know that the sodium is jumping with a characteristic time of the order of $1/\nu_q$, where in this case $\nu_q = (3/2I(2I-1))(e^2qQ/h)$. Scheinert and Weiss[6] have reported e^2qQ/h for sodium as 1.1 MHz with an η value of 0.21. The $1/\nu_q$ value is 2×10^{-6} s. This time is long compared to the characteristic X-ray–matter interaction time but short compared to the X-ray signal integration time. So we do have both kinds of averaging processes acting in the X-ray diffraction analysis.

The jumping process will cause the local ^{27}Al quadrupolar principal axis system to fluctuate, but the mean positions of Al and Cl in $AlCl_4^-$ are only slightly affected. The jumping time of Na^+ is certainly small compared to the reorientation time of $AlCl_4^-$ (this latter statement is not in disagreement with the dimensions of the ellipsoids in Figure 3b).

Now, when the temperature is increased, there is a slight expansion of the structure and increased amplitudes for Na^+ jumps (the mean Na–Cl distances increase; see Figure 2c). However, at some point $AlCl_4^-$ slow motion occurs, sensed by NMR but not by X-rays. Hence, the reorientation time should be short compared to the X-ray integration time and must not change any crystallographic orientation. It cannot be a fully free rotation but a tetrahedral jump rotation. In this case, the positions before and after the jump are not discernible by X-ray diffraction. On the other hand, these orientational jumps will cause Q coordinates to fluctuate compared to B_0, and when the mean reorientational time is of the order of $1/2\nu_q$ for a spin $I = {}^5/_2$, then quadrupolar interactions will average, tending to zero when the reorientation time becomes very short compared to $1/2\nu_q$. It means that when examined by NMR spectroscopy, the jumping process is so fast that every crystallographic equivalent position of $AlCl_4^-$ is visited several times during the NMR experiment. To these reorientations, Na^+ jumps are associated to accommodate the local perturbation. It is not known whether Na^+ jumps may be only local—within the unit cell—or nonlocal. But they contribute also to the fluctuations in Q compared to B_0. So, we can picture the sodium tetrachloroaluminate crystal, as described in the following.

First, at low temperatures (certainly below room temperature), sodium ions start to jump from site to site within the unit cell (like local vibrations with large amplitudes). Then with some increase in temperature, the jumps will go beyond local sites resulting in ionic conductivity.

At this point some positional disorder exists for sodium, though it should not be considered a liquidlike behavior of the cationic lattice because the time taken by the jumps is still short compared to the residence time of Na^+ in the unit cell (in fact, this might also be true for real liquids). These translational motions of Na^+ (or Li^+) are "greasing" the anionic lattice, and when the volume of the unit cell is sufficient, $AlCl_4^-$ will start tetrahedral reorientation, creating orientational disorder. The onset temperature of this kind of reorientational motion is the same for $NaAlCl_4$ and $LiAlCl_4$. This motion seems to be cation-independent but must certainly be slightly lattice-dependent.

Continuous tetrahedral reorientation is completed for $NaAlCl_4$ before loss of long-distance order occurring at fusion. This is not the case for $LiAlCl_4$. These processes are associated with free energy variations that are sensed by calorimetry.

Conclusions

The NMR and X-ray results are completely consistent if we postulate that the librational or rotational motions of the $AlCl_4^-$ groups are not continuous like for a revolving sphere but instead are characterized by a discontinuous reorientational movement, jumping from one stable position to another, resting in these positions much longer than on the way between them.

The structural results are in the trend of the data of the lower temperature structure determinations. On the other hand, our ^{27}Al NMR data (and the conductivity and ^7Li NMR data of the literature) clearly show that transitions take place. It is interesting that we sometimes see a small endothermic effect at 146 °C in the thermal analysis of nonpolycrystalline (virgin) $NaAlCl_4$ samples and that the cryoscopically determined enthalpy of melting is lower than the calorimetric value.

The NMR spectra are explainable by assuming the existence of rotating $AlCl_4^-$ ions at high temperatures. This interpretation is supported by the line-width variations of the signals in the ^{27}Al NMR spectra. The motion is of a discrete type, with symmetry axis of motion coinciding with crystallographic ones.

The liquidlike behavior (conductivity) of Na^+ and Li^+ ions above room temperature within the lattice of $AlCl_4^-$ ions is not considered to come from jumps of a cation from an occupied to a vacant site. Rather, like in liquids, the cations move whenever there is enough collective flexibility in the structure, creating at the same time a defect and a vacant site.

In the course of our study we have been able to recognize some of the steps of motion occurring consecutively during the fusion process of the tetrachloroaluminates of lithium and sodium. Usually all these motions are supposed to occur at the fusion temperature. This was not the case here. Such kind of motion differentiation in melting inorganic crystals, as also discussed in detail by Ubbelohde,[36] could be more frequently occurring than generally recognized.

Acknowledgment. We are in debt to Prof. W. Hoffmann for recording high-temperature photographs and to Prof. N. J. Bjerrum for valuable comments. For financial support, R.W.B.

(33) Weppner, W.; Huggins, R. A. *Phys. Lett.* **1976**, *58A*, 245.
(34) Weppner, W.; Huggins, R. A. *J. Electrochem. Soc.* **1977**, *124*, 35.
(35) Weppner, W.; Huggins, R. A. *Solid State Ionics* **1980**, *1*, 3.
(36) Ubbelohde, A. R. *The molten state of matter*; J. Wiley & Sons: New York, 1978.

is grateful to The Danish Ministry of Energy. B.K., H.G., and C.B. gratefully acknowledge generous support by the Fonds der Chemischen Industrie.

Supplementary Material Available: Tables SIV and SV, listing anisotropic temperature factors and L and T tensors from the librational analysis of $AlCl_4^-$ (2 pages); Tables SI-SIII, listing observed and calculated structure factors of $NaAlCl_4$ at three different temperatures, 138, 150, and 154 °C, respectively (13 pages). Ordering information is given on any current masthead page.

Contribution from the Department of Chemistry, University of Minnesota, Minneapolis, Minnesota 55455

Heterobimetallic Au-Pd Cluster Complexes. X-ray Crystal and Molecular Structures of $[(CO)Pd(AuPPh_3)_8](NO_3)_2$ and $[(P(OCH_3)_3)Pd(AuPPh_3)_6(AuP(OCH_3)_3)_2](NO_3)_2$

Larry N. Ito, Anna Maria P. Felicissimo,† and Louis H. Pignolet*

Received August 24, 1990

In this paper we report the nucleophilic addition/substitution reactions of tertiary phosphites $P(OMe)_3$ and $P(OCH_2)_3CCH_3$ to the 16-electron clusters $[Pd(AuPPh_3)_8]^{2+}$ (**1**) and $[(PPh_3)Pd(AuPPh_3)_6]^{2+}$ (**3**) to give the new 18-electron compounds $[(P(OCH_3)_3Pd(AuPPh_3)_6(AuP(OCH_3)_3)_2]^{2+}$ (**5**) and $[(P(OCH_2)_3CCH_3)_2Pd(AuPPh_3)_6]^{2+}$ (**4**), respectively. These compounds have been characterized by IR spectroscopy, FABMS, and ^{31}P and ^1H NMR spectroscopy. An electrochemical study of **1** has also been carried out. The 16-electron cluster undergoes two reversible single-electron reductions to the neutral 18-electron compound $[Pd(AuPPh_3)_8]^0$. The reaction of **1** and **3** with CO has also been investigated with the result that only **1** gives a product, $[(CO)Pd(AuPPh_3)_8](NO_3)_2$ (**2**). X-ray crystal structure determinations have been carried out on the 18-electron clusters **2** and **5**, and their metal core geometries, which are spheroidal fragments of centered icosahedrons, are in agreement with predictions based on electron counting. The crystal data for these compounds are as follows: for **2**, triclinic $P\bar{1}$, a = 16.23 (1) Å, b = 16.94 (2) Å, c = 30.78 (1) Å, α = 89.63 (6)°, β = 87.61 (5)°, γ = 62.54 (7)°, V = 7496 Å^3, Z = 2, residuals R = 0.075 and R_w = 0.085 for 9559 observed reflections and 718 variables, Mo Kα radiation; for **5**, triclinic $P\bar{1}$, a = 18.577 (3) Å, b = 19.248 (3) Å, c = 21.963 (8) Å, α = 82.00 (2)°, β = 78.16 (2)°, γ = 74.90 (2)°, V = 7390 Å^3, Z = 2, residuals R = 0.060 and R_w = 0.069 for 4465 observed reflections and 346 variables, Mo Kα radiation.

Introduction

Recently, we reported the synthesis and characterization of the first metal cluster compounds that contain Pd-Au bonds.[1] The $NaBH_4$ reduction of a CH_2Cl_2 solution that contains $Pd(PPh_3)_4$ and $Au(PPh_3)NO_3$ led to the formation of $[Pd(AuPPh_3)_8]^{2+}$ (**1**) in good yield and $[(PPh_3)Pd(AuPPh_3)_6]^{2+}$ (**3**) as a minor product. These compounds were separated by HPLC methods. The structure of **1** was determined by single-crystal X-ray diffraction, and the $PdAu_8$ core has a palladium-centered crown or square-antiprismatic geometry similar to that of its Pt analogue.[2] Although a large number of transition-metal-gold phosphine cluster compounds have been prepared,[2-18] there exists a void of well-characterized cluster compounds that contain palladium and gold. In this paper we report an improved synthesis for **1** and **3** that gives the compounds separately and in high yield, as well as the synthesis and characterization of $[(CO)Pd(AuPPh_3)_8]^{2+}$ (**2**) and two new phosphite-containing cluster compounds $[(P(OCH_2)_3CCH_3)_2Pd(AuPPh_3)_6]^{2+}$ (**4**) and $[(P(OCH_3)_3Pd(AuPPh_3)_6(AuP(OCH_3)_3)_2]^{2+}$ (**5**). These compounds form a group of PdAu clusters that show novel structures and interesting reactivity and represent a significant advance in this research area.

The above cluster compounds are palladium centered and can be classified as having 16 or 18 Pd valence electrons. In electron counting for these complexes, the central Pd contributes 10 electrons, each $AuPPh_3$ or $AuP(OR)_3$ unit, 1 electron, and $P(OR)_3$ or CO, 2 electrons. This electron counting has been shown to be useful in predicting reactivity[2,14,15,18] and structure.[19,20] For example, the addition of CO to the 16-electron cluster **1** gives the stable 18-electron adduct **2**.[1] In this paper we show that compound **1** undergoes two reversible single-electron reductions by cyclic voltammetry to the neutral 18-electron cluster $[Pd(AuPPh_3)_8]^0$. A similar electrochemical result has been reported for the isoelectronic 16-electron clusters $[Pt(AuPPh_3)_8]^{2+}$ and $[Au(AuPPh_3)_8]^{3+}$,[21] and a comparison of the data will be made here. In this paper we also report the nucleophilic addition/substitution reactions of tertiary phosphites $P(OMe)_3$ and $P(OCH_2)_3CCH_3$ to the 16-electron clusters $Pd(AuPPh_3)_8^{2+}$ (**1**) and $[(PPh_3)Pd(AuPPh_3)_6]^{2+}$ (**3**), respectively, to give the new 18-electron com-

† Institute of Chemistry, University of São Paulo, São Paulo, Brazil.

(1) Ito, L. N.; Johnson, B. J.; Mueting, A. M.; Pignolet, L. H. *Inorg. Chem.* **1989**, *28*, 2026.
(2) Kanters, R. P. F.; Schlebos, P. P. J.; Bour, J. J.; Bosman, W. P.; Behm, H. J.; Steggerda, J. J. *Inorg. Chem.* **1988**, *27*, 4034. Bour, J. J.; Kanters, R. P. F.; Schlebos, P. P. J.; Bosman, W. P.; Behm, H.; Beurskens, P. T.; Steggerda, J. J. *Recl.: J. R. Neth. Chem. Soc.* **1987**, *106*, 157. Bour, J. J.; Kanters, R. P. F.; Schlebos, P. P. J.; Steggerda, J. J. *Recl.: J. R. Neth. Chem. Soc.* **1988**, *107*, 211.
(3) Mueting, A. M.; Bos, W.; Alexander, B. D.; Boyle, P. D.; Casalnuovo, J. A.; Balaban, S.; Ito, L. N.; Johnson, S. M.; Pignolet, L. H. In *Recent Advances in Di- and Polynuclear Chemistry*; Braunstein, P., Ed. *New J. Chem.* **1988**, *12*, 505 and references cited therein.
(4) Boyle, P. D.; Boyd, D. C.; Mueting, A. M.; Pignolet, L. H. *Inorg. Chem.* **1988**, *27*, 4424.
(5) Alexander, B. D.; Gomez-Sal, M. P.; Gannon, P. R.; Blaine, C. A.; Boyle, P. D.; Mueting, A. M.; Pignolet, L. H. *Inorg. Chem.* **1988**, *27*, 3301.
(6) Bos, W.; Steggerda, J. J.; Shiping, Y.; Casalnuovo, J. A.; Mueting, A. M.; Pignolet, L. H. *Inorg. Chem.* **1988**, *27*, 948.
(7) Boyle, P. D.; Johnson, B. J.; Alexander, B. D.; Casalnuovo, J. A.; Gannon, P. R.; Johnson, S. M.; Larka, E. A.; Mueting, A. M.; Pignolet, L. H. *Inorg. Chem.* **1987**, *26*, 1346.
(8) Smith, E. W.; Welch, A. J.; Treurnicht, I.; Puddephatt, R. J. *Inorg. Chem.* **1986**, *25*, 4616.
(9) Bour, J. J.; Kanters, R. P. F.; Schlebos, P. P. J.; Steggerda, J. J. *Recl. Trav. Chim. Pays-Bas* **1988**, *107*, 211.
(10) Bour, J. J.; Kanters, R. P. F.; Schlebos, P. P. J.; Bos, W.; Bosman, W. P.; Behm, H.; Beurskens, P. T.; Steggerda, J. J. *J. Organomet. Chem.* **1987**, *329*, 405.
(11) Jones, P. G. *Gold Bull.* **1986**, *19*, 46 and references cited therein.
(12) Braunstein, P.; Rosé, J. *Gold Bull.* **1985**, *18*, 17.
(13) Hall, K. P.; Mingos, D. M. P. *Prog. Inorg. Chem.* **1984**, *32*, 237 and references cited therein.
(14) Ito, L. N.; Felicissimo, A. M. P.; Pignolet, L. H. *Inorg. Chem.*, in press.
(15) Kanters, R. P. F.; Schlebos, P. P. J.; Bour, J. J.; Bosman, W. P.; Smits, J. M. M.; Beurskens, P. T.; Steggerda, J. J. *Inorg. Chem.* **1990**, *29*, 324.
(16) Bour, J. J.; Berg, W. V. D.; Schlebos, P. P.; Kanters, R. P. F.; Schoondergang, M. F. J.; Bosman, W. P.; Smits, J. M. M.; Beurskens, P. T.; Steggerda, J. J.; van der Sluis, P. *Inorg. Chem.* **1990**, *29*, 2971.
(17) Kanters, R. P. F.; Bour, J. J.; Schlebos, P. P. J.; Steggerda, J. J. *J. Chem. Soc., Chem. Commun.* **1988**, 1634.
(18) Ito, L. N.; Sweet, J. D.; Mueting, A. M.; Pignolet, L. H.; Schoondergang, M. F. J.; Steggerda, J. J. *Inorg. Chem.* **1989**, *28*, 3696.
(19) Stone, A. J. *Inorg. Chem.* **1981**, *20*, 563.

0020-1669/91/1330-0988$02.50/0